Progress In Electromagnetics Research Letters, Vol. 90, 113–119, 2020

Design of a Triple-Band Antenna Based on Its Current Distribution

Xubao Sun*

Abstract—A triple-band patch antenna operating at 0.9, 1.8 and 2.4 GHz is presented. The triple-band characteristic is realized by using a radiating patch and two meander lines achieved by embedding slots in its radiating patch. According to the current distribution of the radiating patch, the locations of two meander lines are chosen. The proposed antenna has the advantages of the easy control of each resonant frequency and relatively simple antenna structure. The measured −10 dB impedance bandwidths are 30, 40, and 30 MHz at 0.9, 1.8, and 2.4 GHz, respectively. The simulated and measured radiation patterns and gains are also presented and discussed.

1. INTRODUCTION

With the rapid development of modern wireless communication systems, there are increasing requirements for antennas with multi-band operating frequencies in recent years. Patch antennas are good candidates for these applications, because they have small weight and size, low cost, low profile, and ease of fabrication and integration, which are widely used in wireless communication systems. Multi-band patch antennas, in wireless local area network (WLAN) bands at 2.4, 5.2 and 5.8 GHz and worldwide interoperability for microwave access (WiMAX) at 2.5, 3.5 and 5.5 GHz, have been introduced in the literature [1–4]. Various techniques have been reported to achieve multi-band antenna, such as using different slots cut in patch [5, 6], microstrip feed line [7] or ground patch [8, 9], stacked patch [10], and parasitic elements [11]. In [12], a triple-band antenna is presented by using a corner-truncated circular disc sector patch. As a similar technique, in [13], the multi-band performance can be achieved by embedding differently shaped slots in a radiating patch and its ground plane, by properly optimizing sizes and locations of the slots, which result in three resonant frequencies. In triple-band antenna designs, the main challenge is tuning each band independently without affecting the other operating frequencies. In the study by [10], although three independent bands are obtained, the antenna has a relatively complex structure.

In this research, we present a novel triple-band patch antenna operating at 0.9, 1.8, and 2.4 GHz. The three resonant frequencies can serve global systems for mobile communication (GSM), digital communication system (DCS), and wireless local area network (WLAN), respectively. By choosing locations of the slots etched in the patch according to the current distribution of the rectangular patch antenna at 1.8 GHz, the proposed antenna possesses two advantages. First, it is very easy to realize triple-band characteristics, and second, it is a simple antenna structure. Table 1 shows the comparison of antenna operating frequencies and S_{11} between the presented antenna and reported antennas.

2. ANTENNA STRUCTURE

The schematic configuration of the proposed antenna is shown in Fig. 1(a), where the top and side views are presented, and the fabricated prototype is shown in Fig. 1(b). The antenna is printed on an

Received 25 December 2019, Accepted 22 January 2020, Scheduled 14 April 2020
* Corresponding author: Xubao Sun (sunxbcg@163.com).
The author is with the Department of Communication Engineering, College of Electronic Information Engineering, Shandong University of Science and Technology, Qingdao, China.

Table 1. Comparison with reported triple-band antennas.

Antenna	Triple frequencies (GHz)			S_{11}/dB			Frequency differences (GHz)	
	f_1	f_2	f_3	f_1	f_2	f_3	$f_2 - f_1$	$f_3 - f_2$
[5]	2.45	3.5	5.8	−20	−15	−12	1.05	2.2
[6]	2.4	3.6	5.2	−16	−19	−19	1.2	1.6
[10]	1.2	1.6	2.5	−20	−20	−25	0.4	0.9
This work	0.9	1.8	2.4	−35	−45	−25	0.9	0.6

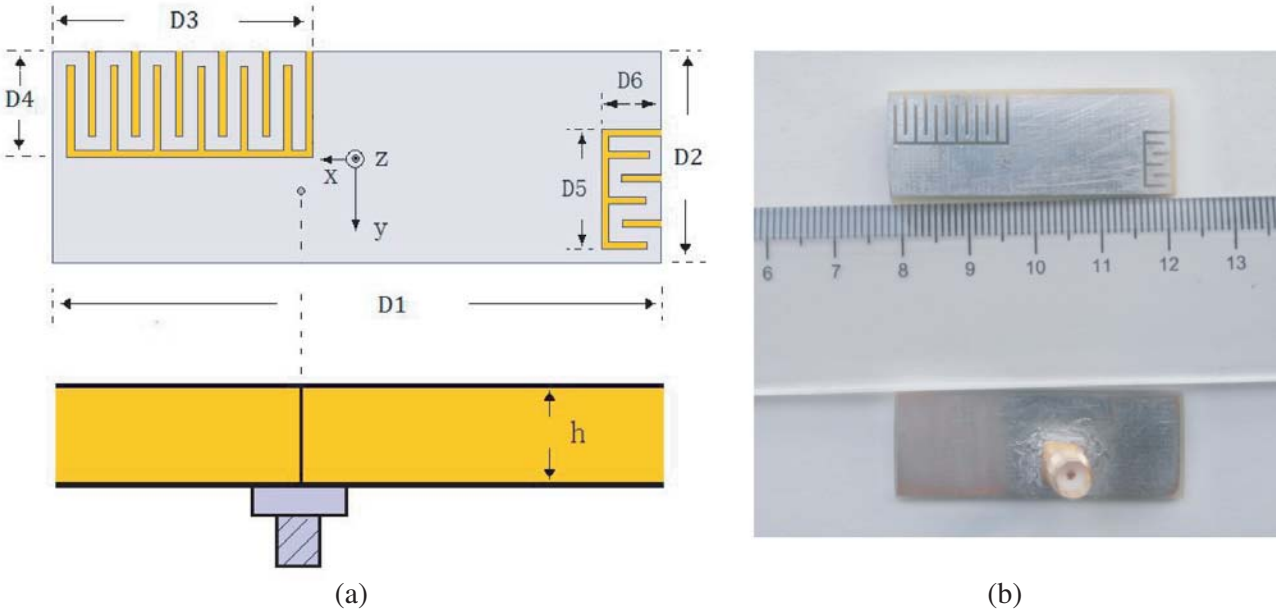

(a) (b)

Figure 1. (a) Schematic diagram of the antenna: top view and side view. (b) Fabricated antenna: top view and bottom view.

FR-4 substrate having height $h = 1.6\,\text{mm}$, dielectric constant 4.4, and loss tangent 0.02. This antenna structure is a rectangular patch with dimensions of $42 \times 15 \times 1.6\,\text{mm}^3$. The antenna is fed by a coaxial cable. By cutting slots on the patch, each slot width is 0.5 mm, and two meander structures are installed on the left top and right bottom of the patch as shown in Fig. 1. The designed and optimized parameter values are as follows: $D1 = 42\,\text{mm}$, $D2 = 15\,\text{mm}$, $D3 = 19.2\,\text{mm}$, $D4 = 7.6\,\text{mm}$, $D5 = 10.6\,\text{mm}$, $D6 = 5.2\,\text{mm}$, $h = 1.6\,\text{mm}$, and the feed point coordinate is ($x = 2.62\,\text{mm}$, $y = 3.37\,\text{mm}$).

3. RESULTS AND DISCUSSION

All parameters of the proposed antenna are simulated and optimized by the software ANSOFT High-Frequency Structure Simulator (HFSS). In order to better explain the working of proposed triple-band radiator, we first introduce the current distribution of a rectangular patch antenna. By optimizing dimensions of the antenna, the rectangular patch antenna with a size $42 \times 15 \times 1.6\,\text{mm}^3$ ($D1 = 42\,\text{mm}$, $D2 = 15\,\text{mm}$, $h = 1.6\,\text{mm}$) is shown in Fig. 2(a); the FR-4 substrate height is 1.6 mm; the dielectric constant is 4.4; loss tangent is 0.02; and its working center frequency is 1.8 GHz. The location of feeding point is at (2.51 mm, 3.1 mm). The current distribution of the rectangular patch antenna is simulated by the HFSS in Fig. 2(b), and we can find that the current mainly concentrates on the center of the patch. Hence, by etching slots on the area of the lowest current, two meander structures are formed as shown in Fig. 1. In general, each length of the meander is about a half wavelength corresponding to its

operating frequency. The evolution of the proposed antenna is described in Fig. 3. Fig. 3(a) shows the rectangular patch antenna, Fig. 3(b) the rectangular patch antenna with meander 1, and Fig. 3(c) the antenna with meander 1 and meander 2. Compared to the antenna in Fig. 3(a), the proposed antenna in Fig. 3(c) provides triple-band performance. Fig. 4 shows the simulated results of the S_{11} with and without meander 1. It can be observed that there are two resonant frequencies at 1.8 and 0.9 GHz by

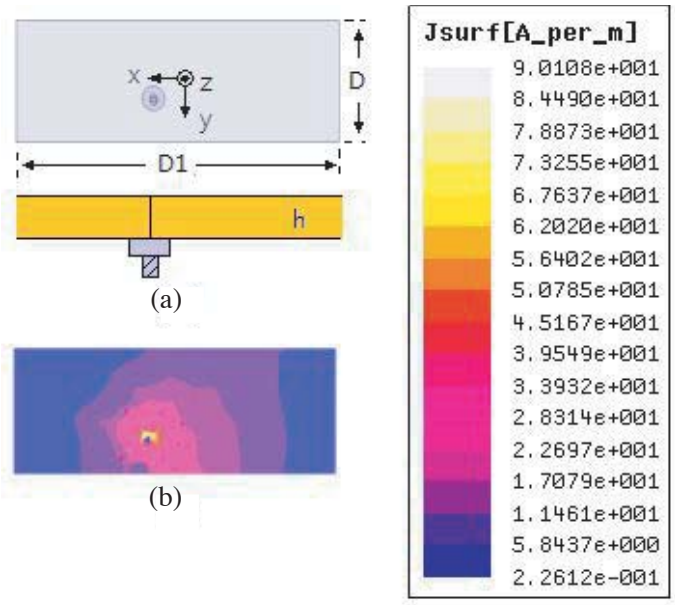

Figure 2. (a) Configuration of the rectangular patch antenna at 1.8 GHz. (b) Current distribution of the rectangular patch antenna at 1.8 GHz.

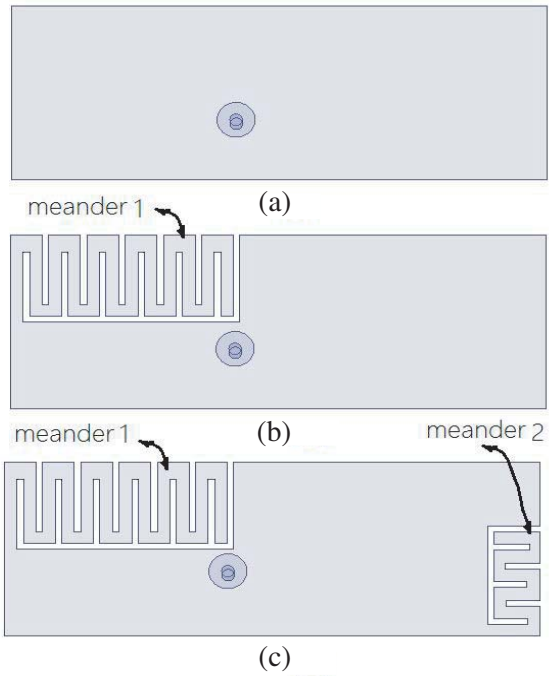

Figure 3. Evolution of the proposed antenna. (a) Stage 1: the rectangular patch antenna at 1.8 GHz. (b) Stage 2: with meander 1. (c) Stage 3: with meander 1 and 2.

adding meander 1, and it can be noted that the resonant frequency 1.8 GHz is almost unaffected. This result is what we expected. Continuing, meander 2 is added in the patch. It is worth mentioning that without tuning other parameter values, we only optimize the location of feeding point for satisfying the requirement of S_{11}, and the optimized result is that a new feeding point moves to $(2.62, 3.37)$ from $(2.51, 3.1)$, and the desirable triple frequency bands are obtained at 0.9, 1.8, and 2.4 GHz, as shown in Fig. 5. Fig. 5 depicts the simulated diagrams of S_{11} with one and two meanders. From ours design procedure, it is obvious that it is very easy to construct three resonant frequencies independently. In other words, the proposed antenna has independent triple-band characteristics, and the three resonant frequencies have almost no interaction with each other. In order to better examine the mechanism of the triple-band antenna, the simulated current distributions on the rectangular patch at 0.9 and 2.4 GHz are depicted in Fig. 6. From Figs. 6(a) and (b), it can be seen that at the lower and higher bands, the current is mainly distributed along the region of meander 1 and the region of meander 2, respectively. Meander 1 is related with GSM band at center frequency 0.9 GHz, whereas meander 2 can control the WLAN band at center frequency 2.4 GHz. The total rectangular patch can control DCS band at center frequency 1.8 GHz.

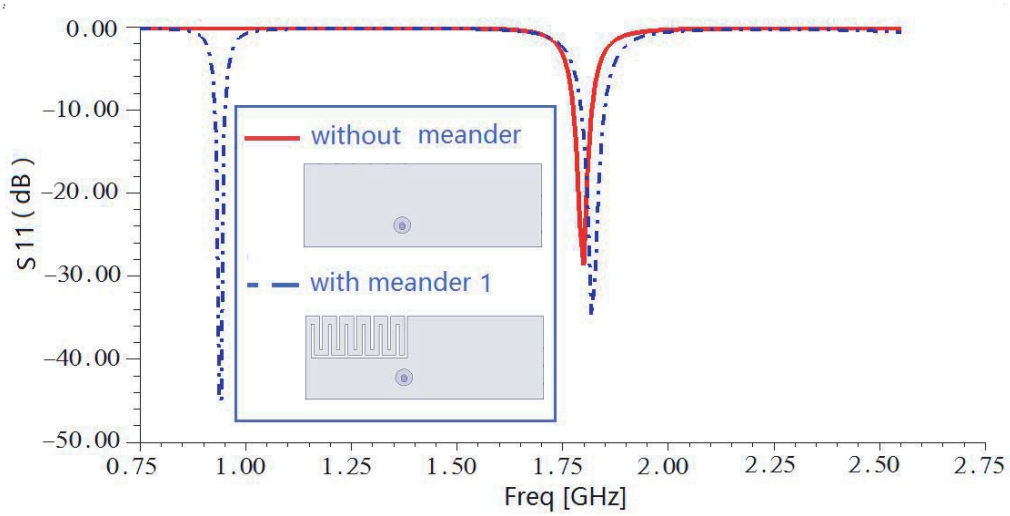

Figure 4. Simulated diagrams of S_{11} with and without one meander.

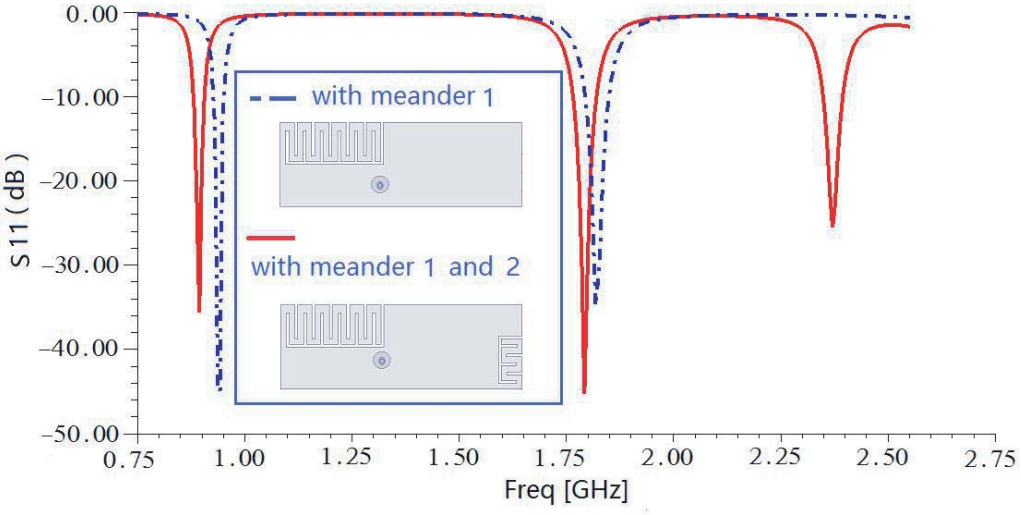

Figure 5. Simulated diagrams of S_{11} with one meander and two meanders.

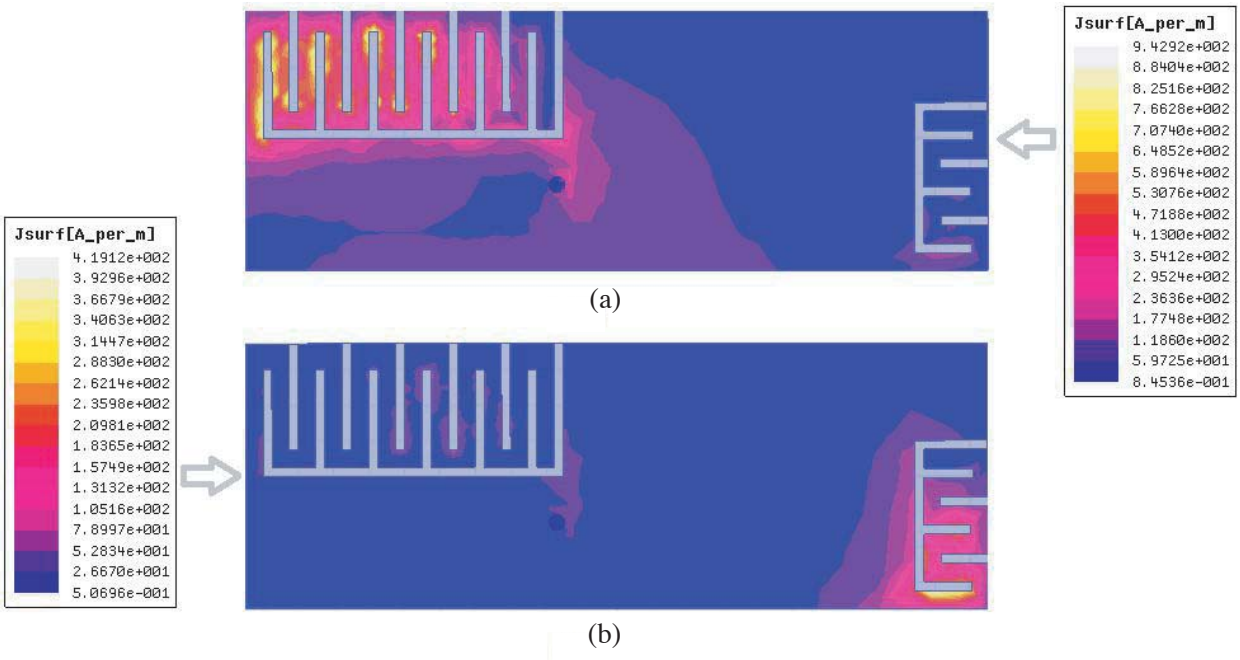

Figure 6. Simulated current distributions. (a) 0.9 GHz, (b) 2.4 GHz.

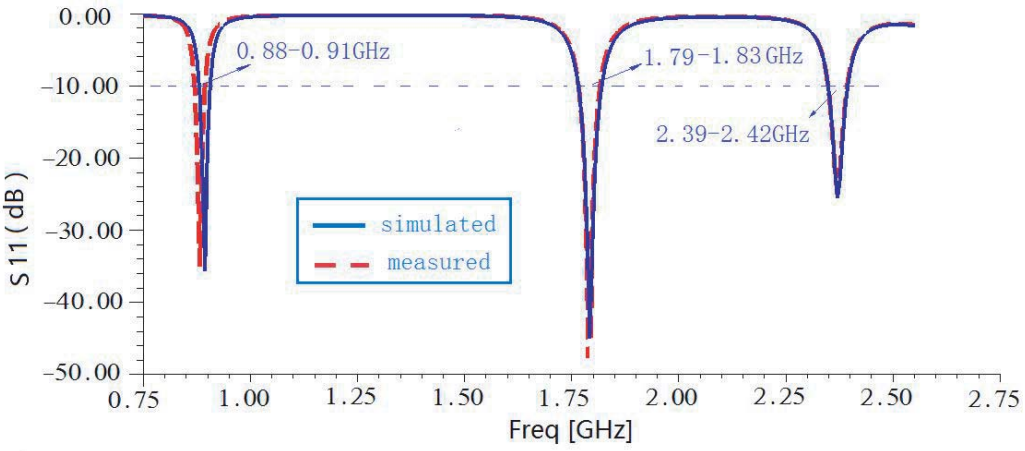

Figure 7. Measured and simulated diagrams of S_{11}.

The final dimensions are based on the proposed antenna, which is fabricated and measured. Fig. 7 shows the measured and simulated results of S_{11}, showing good agreement at the three targeted frequencies. The measured -10 dB impedance bandwidths are 30, 40, and 30 MHz at 0.9, 1.8, and 2.4 GHz, respectively. Although each bandwidth of the proposed triple-band antenna is less than that reported in past [1, 3], these centre frequencies of the proposed antenna are different from their reports. If antenna needs wide bandwidth, it is easy to increase bandwidth by using conventional methods, such as adding slots in patch or ground [14, 15], increasing dielectric thickness and method based monopole antenna [5, 16].

In addition, the far-field radiation patterns of the proposed antenna are also given through measurement in an anechoic chamber. The measured and simulated radiation patterns at 0.9, 1.8, and 2.4 GHz are plotted in Fig. 8. It can be found that the proposed antenna has a good omnidirectional

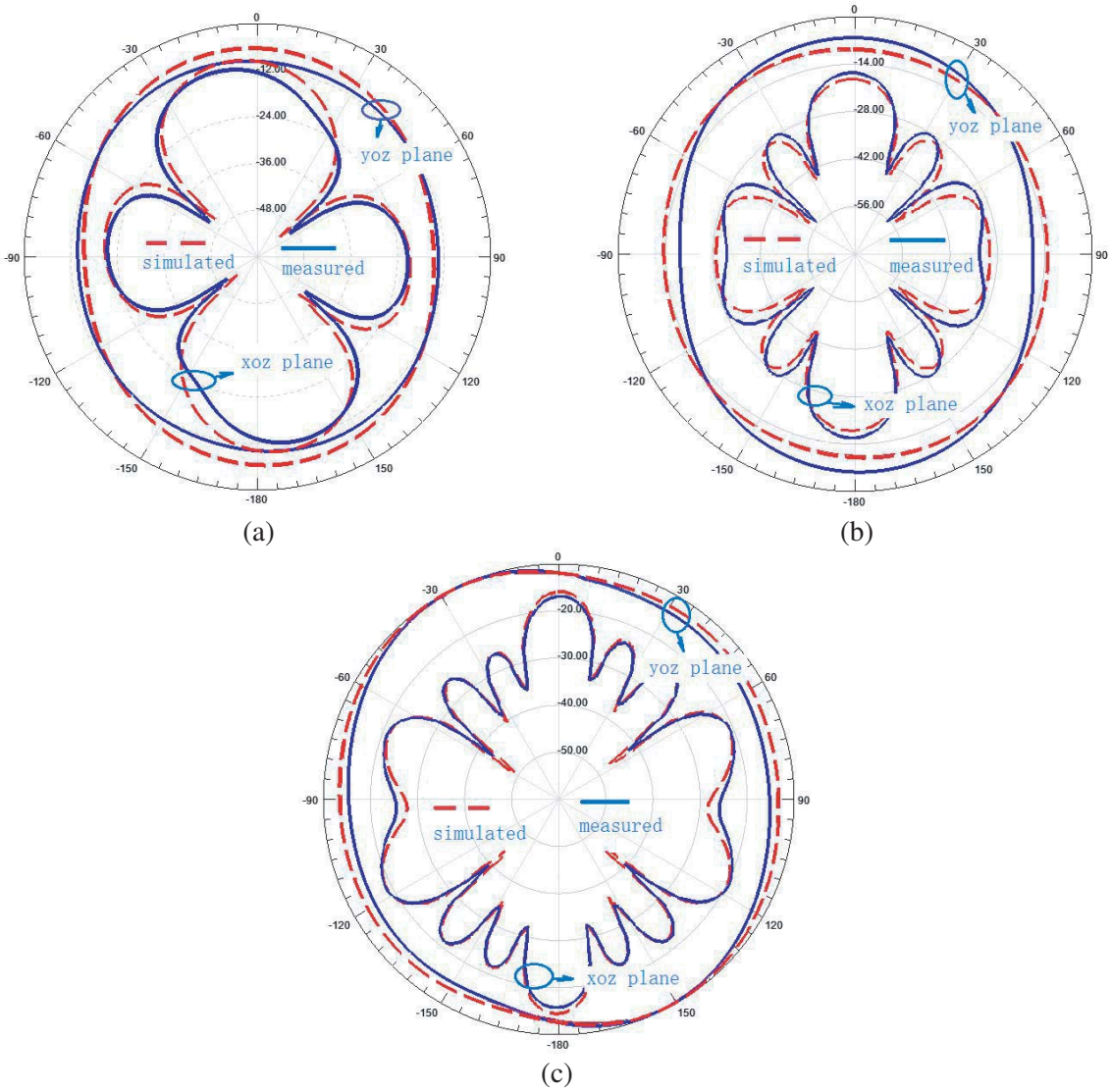

Figure 8. Measured and simulated radiation patterns of the proposed antenna at (a) 0.9 GHz, (b) 1.8 GHz, (c) 2.4 GHz.

radiation pattern in the *yoz*-plane. The measured peak gains are 1.62 dBi, 2.12 dBi, and 1.89 dBi at 0.9, 1.8, and 2.4 GHz, respectively.

Table 1 shows the comparison with reported triple-band antennas. In our work, the frequency difference of the proposed antenna is smaller, and S_{11} is better than antennas.

4. CONCLUSION

In this article, a triple-band microstrip patch antenna for GSM, DCS, and WLAN applications is proposed. The triple-band function is achieved by using two meander structures, and it exhibits independent triple-band characteristics, simple antenna structure, and good radiation performances. All measured results show good agreement with the simulations at the three service bands. The proposed antenna is suitable for wireless communication applications.

REFERENCES

1. Li, L., X. L. Zhang, X. Yin, and L. Zhou, "A compact triple-band printed monopole antenna for WLAN/WiMAX applications," *IEEE Antennas and Wireless Propagation Letters*, Vol. 15, 853–1855, 2016.
2. Sung, Y., "Triple band-notched UWB planar monopole antenna using a modified H-shaped resonator," *IEEE Transactions on Antennas and Propagation*, Vol. 61, No. 2, 953–957, 2013.
3. Kunwar, A., A. K. Gautam, and K. Rambabu, "Design of a compact U-shaped slot triple band antenna for WLAN/WiMAX applications," *AEU — International Journal of Electronics and Communications*, Vol. 71, 82–88, 2017.
4. Reddy, V. V. and N. V. S. N. Sarma, "Triband circularly polarized koch fractal boundary microstrip antenna," *IEEE Antennas and Wireless Propagation Letters*, Vol. 13, 1057–1060, 2014.
5. Hoang, V. and H. C. Park, "Very simple 2.45/3.5/5.8 GHz triple-band circularly polarised printed monopole antenna with bandwidth enhancement," *IET Electronics Letters*, Vol. 50, No. 24, 1792–1793, 2014.
6. Kumar, A., "A compact H-shaped slot triple-band microstrip antenna for WLAN and WiMAX applications," *IEEE Annual India Conference (INDICON)*, 1–4, 2016.
7. Yadav, A., S. Agrawal, and R. P. Yadav, "SRR and S-shape slot loaded triple band notched UWB antenna," *AEU — International Journal of Electronics and Communications*, Vol. 79, 192–198, 2017.
8. Mansouri, Z., A. S. Arezoomand, S. Heydari, and F. B. Zarrabi, "Dual notch UWB fork monopole antenna with CRLH metamaterial load," *Progress In Electromagnetics Research*, Vol. 65, 111–119, 2016.
9. Salih, A. A. and M. S. Sharawi, "A dual-band highly miniaturized patch antenna," *IEEE Antennas and Wireless Propagation Letters*, Vol. 15, 1783–1786, 2016.
10. Li, L., Y. Huang, L. Zhou, and F. Wang, "Triple-band antenna with shorted annular ring for high-precision GNSS applications," *IEEE Antennas and Wireless Propagation Letters*, Vol. 15, 942–945, 2016.
11. Shen, S., C.-Y. Chiu, and R. D. Murch, "A dual-port triple-band L-probe microstrip patch rectenna for ambient RF energy harvesting," *IEEE Antennas and Wireless Propagation Letters*, Vol. 16, 3071–3074, 2017.
12. Mathew, S., R. Anitha, U. Deepak, and C. K. Aanandan, "A compact tri-band dual-polarized corner-truncated sectoral patch antenna," *IEEE Transactions on Antennas and Propagation*, Vol. 63, No. 12, 5842–5845, 2015.
13. Boukarkar, A., X. Q. Lin, et al. "A highly integrated independently tunable triple-band patch antenna," *IEEE Antennas and Wireless Propagation Letters*, Vol. 16, 2216–2219, 2017.
14. Dutta, S., K. Kumari, D. Sarkar, and K. V. Srivastava, "A compact triple-band multi-polarized slot antenna for WLAN/WiMAX application," *3rd International Conference on Microwave and Photonics (ICMAP 2018)*, 1–2, February 9–11, 2018.
15. Ali, T. and R. C. Biradar, "A miniaturized volkswagen logo UWB antenna with slotted ground structure and metamaterial for GPS, WiMAX and WLAN applications," *Progress In Electromagnetics Research C*, Vol. 72, 29–41, 2017.
16. Brar, R. S., K. Saurav, D. Sarkar, and K. V. Srivastava, "A triple band circular polarized monopole antenna for GNSS/UMTS/LTE," *Microwave and Optical Technology Letters*, Vol. 59, No. 2, 298–304, 2017.